

Magnetic correlations in the disordered ferromagnetic alloy Ni-V revealed with small angle neutron scattering

A. Schroeder,^{1, a)} S. Bhattarai,¹ A Gebretsadik,^{1, b)} H. Adawi,¹ J.-G. Lussier,¹ and K. L. Krycka²

¹⁾Department of Physics, Kent State University, Kent OH 44242, USA

²⁾National Institute of Standards and Technologies, NIST Center of Neutron Research, Gaithersburg MD 20899, USA

(Dated: 10 January 2020)

We present small angle neutron scattering (SANS) data collected on polycrystalline $\text{Ni}_{1-x}\text{V}_x$ samples with $x \geq 0.10$ with confirmed random atomic distribution. We aim to determine the relevant length scales of magnetic correlations in ferromagnetic samples with low critical temperatures T_c that show signs of magnetic inhomogeneities in magnetization and μSR data. The SANS study reveals signatures of long-range order and coexistence of short-range magnetic correlations in this randomly disordered ferromagnetic alloy. We show the advantages of a polarization analysis in identifying the main magnetic contributions from the dominating nuclear scattering.

Formation of ferromagnetism in metals is still an active field for discovery of novel phases and mechanisms in condensed matter physics¹. In particular, the control of disorder and determination of how inhomogeneities affect magnetic properties remains a significant challenge. Small angle neutron scattering (SANS) is one of the prime methods² to characterize magnetic material at the nanoscale. It has revealed important insight in the complex structure formation of inhomogeneous magnets with defects or internal structures from bulk alloys³ to amorphous and nanocrystalline magnetic materials^{2,4}. In this study we focus on the binary transition metal alloy $\text{Ni}_{1-x}\text{V}_x$, that presents an example of a diluted inhomogeneous ferromagnet produced by random atomic distribution^{5,6}. The onset of ferromagnetic order of Ni at $T_c = 630$ K is suppressed towards zero with sufficient V concentration of $x_c = 0.116$ ⁷. Previous magnetization and μSR studies show signatures of fluctuating clusters⁷ from Ni-rich regions for paramagnetic samples with $x > x_c$. These persist also into the ferromagnetic state close to x_c and coexist with the static order⁵ evolving below T_c . With SANS we aim to measure the magnetic cluster sizes and their effect on the static order in this random disordered system. We present a SANS study with polarization analysis⁸ to extract magnetic scattering that would otherwise be dominated by nuclear scattering.

For this study we used the same polycrystalline samples of $\text{Ni}_{1-x}\text{V}_x$ that were prepared for optimal random distribution and characterized by several methods⁶ from previous studies^{5,7}. Several pellets of 3 mm diameter of each concentration were wrapped in Al foil and mounted on Al- sample holder framed with Cd-mask and connected to the cold plate of the cryostat. The SANS experiments were performed at GPSANS, HFIR, Oak Ridge National Lab and at NG7SANS⁹, NCTR, NIST. We show detailed data from NIST of $\text{Ni}_{0.90}\text{V}_{0.10}$ samples using also polarized neutrons (tracking the polarization (p) state before and after sample). The SANS intensity was collected in the xy -plane on a 2D

detector at different distances to cover a wave vector (Q)-range of $(0.06-1) \text{ nm}^{-1}$ with neutron wavelengths of 0.55 nm and 0.75 nm. Taking advantage of supermirror polarizer and ³He-cell as spin analyser as described in detail before^{10,11} we collected separately non spin flip (NSF) scattering with unchanged p-state of the neutrons (DD and UU) and spin flip (SF) scattering with reversed p-state (DU and UD) from the sample. U, D refers to the neutron spins aligned UP, DOWN with respect to the neutron polarization axis defined by the external magnetic field. The magnetic field was applied in the x -direction ($B_{max} = 1.5$ T, $B_{min} = 7$ mT) perpendicular to the beam ($\parallel z$). θ indicates the azimuthal angle within the xy -plane, with $\theta = 0^\circ$ in the horizontal x -direction. Horizontal or vertical data averages included a symmetric cone of width $\pm\Delta\theta = 30^\circ$ around $\theta = 0^\circ$ and 180° or $\theta = \pm 90^\circ$ presented as SFH or SFV, respectively. Besides fully polarization-analyzed PASANS we collected also unpolarized or "non pol" data (NP) without tracking the p-state and "half pol" (HP) data without distinguishing the p-state after the sample (D and U) without a ³He-cell in the beam. The PASANS data were polarization corrected and reduced with the IGOR software¹².

First SANS studies of $\text{Ni}_{1-x}\text{V}_x$ could not resolve the weak magnetic scattering for paramagnetic samples with $x = 0.12$ but recent SANS data collected at NG7SANS, NIST and GP-SANS, ORNL revealed a clear temperature-dependent signal in weak ferromagnetic samples with $x \leq 0.11$ ¹³ that demonstrated that magnetic scattering can be resolved for ferromagnetic samples with a reduced average moment per Ni of $\mu \approx 0.03 \mu_B$ ⁵. We show here the SANS data for $x = 0.10$ with $T_c \approx 50$ K collected at NIST to compare best full pol and non pol data. Fig. 1(a) presents the non polarized neutron scattering intensity as a function of the magnitude of the wavevector Q collected as horizontal average NPH . NPH collects only transverse magnetic contributions M_y^2 and M_z^2 (not the longitudinal magnetic components M_x^2 along the field direction) beside the dominating nuclear contribution N^2 and other backgrounds BG_{NP} .

$$NPH = NP(\theta = 0^\circ) = N^2 + M_z^2 + M_y^2 + BG_{NP} \quad (1)$$

The "non-magnetic" contributions are estimated by NPH col-

^{a)}Electronic mail: aschroe2@kent.edu

^{b)}Present address: Intel, Chandler AZ, USA

lected in high fields ($NPH(B = 1.5 \text{ T}, T < T_c)$) where aligned magnetic moments are expected to contribute only to the magnetic scattering in field direction M_x^2 not to the selected transverse components. The NPH difference of the total non pol scattering collected at different temperatures in low fields ($B = 7 \text{ mT}$) and the high field data should finally reveal the *magnetic scattering* ($M_z^2 + M_y^2$) as shown in Fig. 1(a).

Most magnetic scattering is found close to $T_c \approx 50 \text{ K}$ in the higher Q range ($0.2 \text{ nm}^{-1} - 1 \text{ nm}^{-1}$). It can be approximated by a Lorentzian as expected for paramagnetic critical scattering of the Ornstein Zernike form with a correlation length $1/\kappa$ increasing towards T_c . Below T_c the magnetic intensity is significantly reduced in the higher Q regime, and in addition, an increase of intensity at low Q is noticed that follows a $1/Q^4$ dependence without any sign of saturation.

$$I_{\text{mag}}(Q) = \frac{D}{Q^4} + \frac{L}{\kappa^2 + Q^2} \times F(Q) \quad (2)$$

The fit can be improved somewhat towards higher Q by a form factor¹⁴ $F(Q) = \exp(-\frac{1}{5}r_0^2Q^2)$ with radius $r_0 \approx 1 \text{ nm}$ that could indicate non-uniform magnetic scattering centers or be an artifact of non ideal background subtraction. Different than in homogeneous systems with a narrow critical regime with diverging correlations at T_c typically observed with SANS¹⁵ we find reduced length scales as seen in inhomogeneous ferromagnets² e.g. in diluted ferromagnetic alloys^{3,16} or diluted manganites¹⁷. The correlation length of the visible magnetic contribution remains finite at T_c ($1/\kappa \approx 5 \text{ nm}$) and even seems to grow further below T_c at 30 K. At very low $T = 3 \text{ K}$ we still recognize similar transverse magnetic contributions as observed for T_c with reduced amplitude but similar correlation length. This indicates that short-range fluctuations of the paramagnetic state are still left in the ferromagnetic state at low temperatures. The low- Q upturn in the non pol data (NPH) is most likely due to the contrast of misaligned magnetic regions (domains) of a large scale ($> 100 \text{ nm}$) expected in a soft magnet of finite size at small fields. This domain term becomes apparent below T_c indicating the onset of long-range order. However, it is difficult to extract the magnetic response from the huge nuclear $1/Q^4$ term due to grain boundaries in these polycrystalline samples.

Encouraged by these promising findings of sufficient magnetic scattering in the larger Q regime¹³, but uncertain about reasonable background estimates, we collected full polarized SANS. The clear advantage is the collection of pure spin flip (SF) data (DU+UD) recognizing electronic magnetic scattering through the angle θ dependence⁸ at constant Q .

$$SF(\theta) = M_z^2 + M_y^2 \cos^4 \theta + M_x^2 \cos^2 \theta \sin^2 \theta + BG_{SF} \quad (3)$$

We noticed signs of anisotropy only in field direction $M_x > 0$ (see below) and did not consider transverse terms, $M_y = M_z = 0$ simplifies the spin flip intensity⁸ $SF(\theta)$ in Eq. (3). Fig. 2 presents the angle dependence of the SF data collected for a medium Q range, ($0.2 - 0.5 \text{ nm}^{-1}$), for $\text{Ni}_{0.90}\text{V}_{0.10}$ after a constant background has been subtracted. The solid lines represent fits using Eq. (3) that yield M_y^2 but also M_x^2 with less precision as presented in Fig. 3(a). At high temperatures and

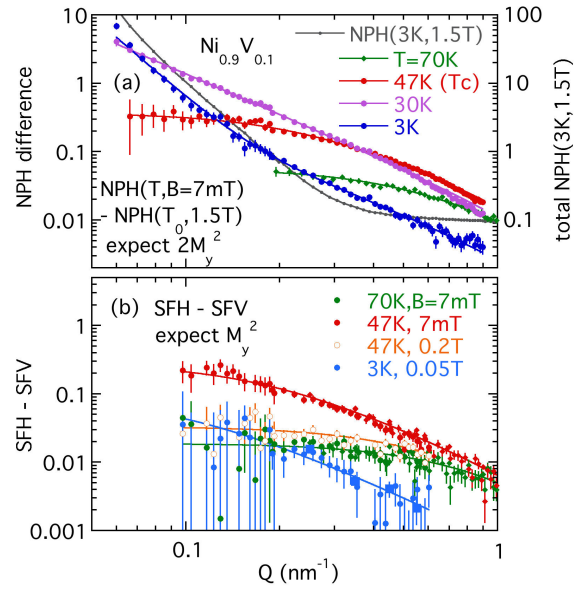


FIG. 1. Magnetic neutron scattering intensity of $\text{Ni}_{0.90}\text{V}_{0.10}$ vs wave vector Q . (a) shows non polarized horizontal averaged data NPH collected at different temperatures in low fields (7 mT) after BG subtraction of high field data, shown separately on a different scale. (b) shows polarized intensity, the spin flip contrast $SFH - SFV$ for different temperatures and magnetic fields indicated. Solid lines present fits using Eq. (2).

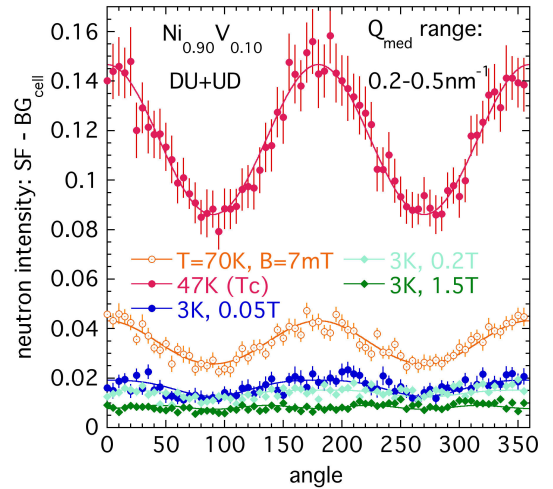


FIG. 2. Spin flip (SF) intensity of $\text{Ni}_{0.90}\text{V}_{0.10}$ vs angle θ at constant Q (average over Q range from 0.2 nm^{-1} to 0.5 nm^{-1}) at different temperatures T and magnetic fields B ($\theta = 0$). Solid lines are fits using Eq. (3).

very small magnetic fields $SF(\theta)$ follows a pure $\cos^2 \theta$ dependence with $M_x^2 = M_y^2$ expected for isotropic paramagnetic fluctuations. The data confirm also that $M_z^2 = M_y^2$. At low $T = 3 \text{ K}$ the SF data are shown for 50 mT and higher fields. At smaller fields the ferromagnetic sample (below T_c) depolarizes the neutron beam that PASANS cannot be analyzed.

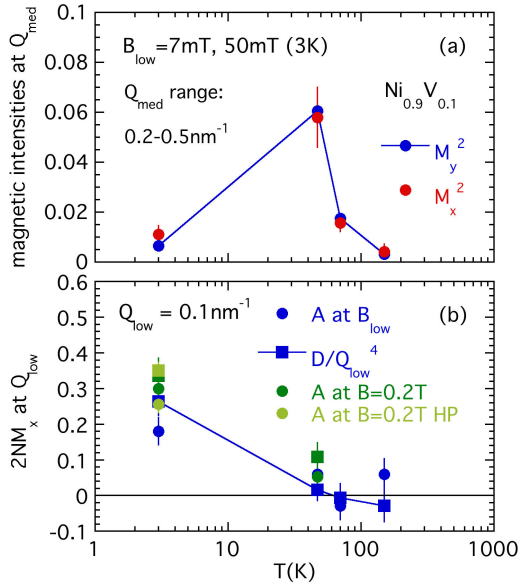


FIG. 3. (a) Temperature (T) dependence of magnetic components M_y^2 and M_x^2 at $Q_{\text{med}} \approx 0.35 \text{ nm}^{-1}$ from fit of Eq. (3) (see Fig. 2) tracing the evolution of magnetic clusters in $\text{Ni}_{0.90}\text{V}_{0.10}$. (b) T dependence of the interference term $2NM_x$ at $Q_{\text{low}} \approx 0.1 \text{ nm}^{-1}$ indicating the evolution of long-range magnetic domains. D/Q_{low} is evaluated from $DIFV(Q)$ with Eq. (2) and A is maximum value in $DIF(\theta)$ using Eq. (4) (see Fig. 4).

The magnetic signal M_y^2 at 3 K in 50 mT is reduced to about 10% of M_y^2 at T_c . M_x^2 is still similar to M_y^2 in small fields. In higher fields M_y^2 gets suppressed to reach very small values for 1.5 T. The confirmed isotropy underlines the fact that these short-range correlations stem from dynamic fluctuations that cold neutrons can collect up to the order of THz especially on smaller ranges. These SF data demonstrate that indeed a small fraction of magnetic fluctuations remain at low temperatures, that get further suppressed in higher magnetic fields.

Fig. 1(b) shows the Q dependence of the SF contrast, SFH-SFV, that evaluates M_y^2 . Since the magnetic response is isotropic for low fields this signal represents (1/3 of) the total magnetic fluctuations M_{tot}^2 . In this restricted Q regime a Lorentzian describes the data well. A finite $r_0 \approx 1 \text{ nm}$ also improves the fit somewhat for large Q . We did not aim to get more detailed nanostructures from these data using alternative descriptions including cluster distributions¹⁸. The Lorentzian fit produces a correlation lengths for 47 K in the order of 7 nm that is similar at $T = 3 \text{ K}$ in 50 mT. The estimate of $1/\kappa \approx (10 \pm 4) \text{ nm}$ includes uncertainties caused by background variations contaminating the small magnetic signal that is resolved in a limited Q regime. Comparing panel (a) and (b) in Fig. 1 we see that the SF data confirm the non polarized magnetic estimates of fluctuations with similar magnitude (M_y^2) and length scales for common data sets in the higher Q regime. But below $Q = 0.1 \text{ nm}^{-1}$ the smaller SF data are difficult to resolve from dominating NSF data after polarization corrections and do not reveal the signatures of

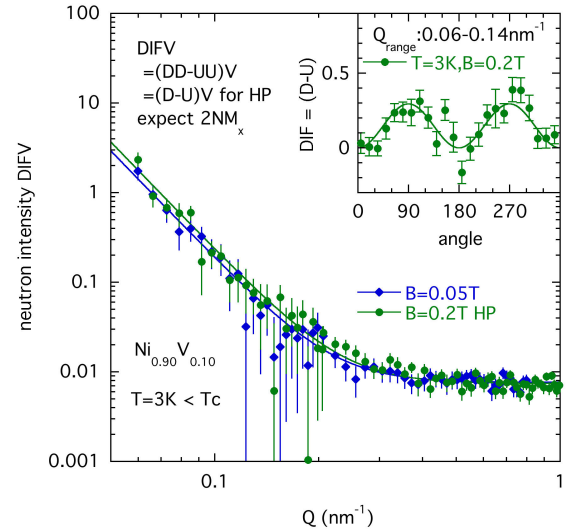


FIG. 4. DIF or flipper difference from full pol NSF data (DD-UU) and half pol data (D-U) to reveal interference term $2NM_x$ indicating magnetic anisotropy with positive M_x in $\text{Ni}_{0.90}\text{V}_{0.10}$ for low $T = 3 \text{ K}$ in magnetic fields of 0.05 T and 0.2 T. The main panel shows the Q dependence of $DIFV$. Solid lines follow Eq. (2) with large κ . The inset presents the θ dependence of DIF at $Q_{\text{low}} \approx 0.1 \text{ nm}^{-1}$. The solid line is a fit that follows Eq. (4).

long-range order. If the $1/Q^4$ upturn in the NPH difference is real magnetic scattering or an artifact of a nuclear origin or multiple scattering cannot be resolved with SF scattering and needs a different approach.

We cannot use the total non spin flip data, NSF, (DD+UU) to reveal the longitudinal magnetic component M_x^2 from the angular dependence⁸ since the nuclear scattering is dominating the signal. But we can take advantage of the difference response “ DIF ” between the two initial polarization direction (without registering spin flip), the NSF asymmetry or flipper difference from full pol data (DD-UU) and HP data (D-U) that yields an interference term of nuclear and magnetic origin⁸. It signals a weak contribution from a center with a net magnetic component along the x -direction $M_x > 0$ in the presence of a strong nuclear contribution from the same center.

$$DIF(\theta) = 2NM_x \sin^2 \theta \quad (4)$$

$DIF(\theta)$ is shown in the inset of Fig. 4 presenting the two maxima at $DIFV = 2NM_x$ according to Eq. (4). Even in the low Q regime this structure can be resolved at low $T = 3 \text{ K}$ in sufficient high fields ($B \geq 50 \text{ mT}$). As shown in the main panel $DIF(Q) = 2NM_x(Q)$ can be presented by a $1/Q^4$ term and a small constant following Eq. (2) with a large parameter κ . Since such Q dependence is expected for nuclear scattering N^2 dominated by large grain boundaries we conclude a similar Q dependence for $(M_x)^2$. Potential deviations of the form $1/(K^2 + Q^2)^2$ yield magnetic domain sizes larger than $1/K \approx 50 \text{ nm}$. Fig. 3(b) presents the estimates of $2NM_x$ collected at different temperatures from

the angle dependence (A) and the Q dependence (D/Q_m^4) at low $Q \approx 0.1 \text{ nm}^{-1}$, $2NM_x \neq 0$ for $T < T_c$ while $2NM_x \approx 0$ for $T \geq T_c$. This interference term $DIFV$ succeeds to resolve magnetic scattering expected for aligned ferromagnetic magnetic domains that form below T_c . The $1/Q^4$ dependence of $(M_x)^2$ reveals long-range magnetic domains. Simple estimates¹⁹ from neutron depolarization yield domain scales of micrometers at $T = 3 \text{ K}$. We expect that in a ferromagnet below T_c fluctuations turn into long-range order, but in this inhomogeneous compound short-range fluctuations are more dominant than in defect-free, homogeneous systems. On one hand random defects produce distinct short-range correlations that are noticed at T_c and are still present at low temperatures but on the other hand they do not destroy long-range order in this alloy.

Collecting SANS data with and without polarization analysis we gained new insight in the inhomogeneous ferromagnetic state of $\text{Ni}_{1-x}\text{V}_x$ with low critical temperatures T_c below 50 K. In this paper we focus on $\text{Ni}_{0.90}\text{V}_{0.10}$. We found clear evidence of magnetic fluctuations in the larger Q regime from spin flip (SF) contrast. From the magnetic fluctuations at T_c a fraction of 10% remains at the lowest temperature of $T = 3 \text{ K}$ with similar correlation lengths of about 10 nm. In addition, the non spin flip (NSF) asymmetry (from full pol and half pol data) reveals large scale aligned magnetic domains in the lower Q regime at low temperatures $T = 3 \text{ K}$ below T_c . Although these random defects cause short-range magnetic fluctuating clusters, long-range order still develops in this alloys. Similar features can be observed in $\text{Ni}_{1-x}\text{V}_x$ samples with $x = 0.11$ with smaller $T_c \approx 7 \text{ K}$. The challenge to resolve the smaller magnetic contribution from the overwhelming nuclear background is increased, but magnetic fluctuations remain and indication of aligned domains are present for low temperatures below T_c . More details will be presented elsewhere¹³. We demonstrated that PASANS is a helpful method to clarify signatures of random dilution in alloys presenting magnetic correlations that persist in a wide range of length scales at low temperatures.

We thank J. Kryzwon, T. Dax, S. Watson and T. Hassan for their support with NG7SANS, cryogenics and ^3He cell spin filters preparation at NIST. Support for usage of the ^3He spin polarizer on the NG7 SANS instrument was provided by the Center for High Resolution Neutron Scattering, a partnership between the National Institute of Standards and Technology and the National Science Foundation under Agreement No. DMR-1508249. This research is funded in part by a QuantEmX grant from ICAM and the Gordon and Betty Moore Foundation through Grant GBMF5305 to Hector D. Rosales. We thank Lisa DeBeer-Schmitt for her support at GPSANS, ORNL. A portion of this research used resources at the High Flux Isotope Reactor, which are DOE Office of Science User

Facilities operated by Oak Ridge National Laboratory.

- ¹M. Brando, D. Belitz, F. M. Grosche, and T. R. Kirkpatrick, "Metallic quantum ferromagnets," *Rev. Mod. Phys.* **88**, 025006 (2016).
- ²S. Mühlbauer, D. Honecker, E. A. Périgo, F. Bergner, S. Disch, A. Heineemann, S. Erokhin, D. Berkov, C. Leighton, M. R. Eskildsen, and A. Michels, "Magnetic small-angle neutron scattering," *Rev. Mod. Phys.* **91**, 015004 (2019).
- ³B. H. Verbeek, G. J. Nieuwenhuys, J. A. Mydosh, C. van Dijk, and B. D. Rainford, "Inhomogeneous ferromagnetic ordering in PdFe and PdMn alloys studied via small-angle neutron scattering," *Phys. Rev. B* **22**, 5426–5440 (1980).
- ⁴A. Michels and J. Weissmüller, "Magnetic-field-dependent small-angle neutron scattering on random anisotropy ferromagnets," *Reports on Progress in Physics* **71**, 066501 (2008).
- ⁵R. Wang, A. Gebretsadik, S. Ubaid-Kassis, A. Schroeder, T. Vojta, P. J. Baker, F. L. Pratt, S. J. Blundell, T. Lancaster, I. Franke, J. S. Möller, and K. Page, "Quantum Griffiths phase inside the ferromagnetic phase of $\text{Ni}_{1-x}\text{V}_x$," *Phys. Rev. Lett.* **118**, 267202 (2017).
- ⁶A. Gebretsadik, R. Wang, A. Alyami, J.-G. Lussier, A. Schroeder, and K. Page, "Study of atomic disorder in Ni-V," to be published.
- ⁷S. Ubaid-Kassis, T. Vojta, and A. Schröder, "Quantum Griffiths phase in the weak itinerant ferromagnetic alloy $\text{Ni}_{1-x}\text{V}_x$," *Phys. Rev. Lett.* **104**, 066402 (2010).
- ⁸K. Krycka, J. Borchers, Y. Ijiri, R. Booth, and S. Majetich, "Polarization-analyzed small-angle neutron scattering. II. Mathematical angular analysis," *Journal of Applied Crystallography* **45**, 554–565 (2012).
- ⁹C. J. Glinka, J. G. Barker, B. Hammouda, S. Krueger, J. J. Moyer, and W. J. Orts, "The 30 m Small-Angle Neutron Scattering Instruments at the National Institute of Standards and Technology," *Journal of Applied Crystallography* **31**, 430–445 (1998).
- ¹⁰K. Krycka, R. Booth, J. Borchers, W. Chen, C. Conlon, T. Gentile, C. Hogg, Y. Ijiri, M. Laver, B. Maranville, S. Majetich, J. Rhyne, and S. Watson, "Resolving 3d magnetism in nanoparticles using polarization analyzed sans," *Physica B: Condensed Matter* **404**, 2561–2564 (2009).
- ¹¹W. Chen, R. Erwin, J. M. III, S. Watson, C. Fu, T. Gentile, J. Borchers, J. Lynn, and G. Jones, "Applications of ^3He neutron spin filters at the NCNr," *Physica B: Condensed Matter* **404**, 2663–2666 (2009).
- ¹²S. R. Kline, "Reduction and analysis of SANS and USANS data using IGOR Pro," *Journal of Applied Crystallography* **39**, 895–900 (2006).
- ¹³S. Bhattarai, A. Gebretsadik, H. Adawi, J.-G. Lussier, A. Schroeder, K. Krycka, and L. Debeer-Schmitt, "SANS study of ferromagnetic alloy Ni-V close to the quantum critical point," to be published.
- ¹⁴D. Saurel, C. Simon, A. Pautrat, C. Martin, C. Dewhurst, and A. Brûlet, "Evolution of the conducting phase topology at the percolation threshold in colossal magnetoresistance manganites: A magnetic small-angle neutron scattering study," *Phys. Rev. B* **82**, 054427 (2010).
- ¹⁵J. W. Lynn, L. Vasiliu-Doloc, and M. A. Subramanian, "Spin dynamics of the magnetoresistive pyrochlore $\text{Tl}_2\text{Mn}_2\text{O}_7$," *Phys. Rev. Lett.* **80**, 4582–4585 (1998).
- ¹⁶S. K. Burke, R. Cywinski, E. J. Lindley, and B. D. Rainford, "Magnetic correlations near the critical concentration in Pd Ni alloys," *Journal of Applied Physics* **53**, 8079–8081 (1982).
- ¹⁷J. M. De Teresa, C. Ritter, P. A. Algarabel, S. M. Yusuf, J. Blasco, A. Kumar, C. Marquina, and M. R. Ibarra, "Detailed neutron study of the crossover from long-range to short-range magnetic ordering in $(\text{Nd}_{1-x}\text{Tb}_x)_{0.55}\text{Sr}_{0.45}\text{MnO}_3$ manganites," *Phys. Rev. B* **74**, 224442 (2006).
- ¹⁸R. G. Calderón, L. F. Barquín, S. N. Kaul, J. C. Gómez Sal, P. Gorria, J. S. Pedersen, and R. K. Heenan, "Small-angle neutron scattering study of a magnetically inhomogeneous amorphous alloy with reentrant behavior," *Phys. Rev. B* **71**, 134413 (2005).
- ¹⁹S. M. Yusuf, M. Sahana, M. S. Hegde, K. Dörr, and K.-H. Müller, "Evidence of ferromagnetic domains in the $\text{La}_{0.67}\text{Ca}_{0.33}\text{Mn}_{0.9}\text{Fe}_{0.1}\text{O}_3$ perovskite," *Phys. Rev. B* **62**, 1118–1123 (2000).